Optimization The Characteristics of Solar Cell based on InGaN

S.Nour [1], A. Merabti [2], H. Issani [3], R. Abdeldjebar [4], A.Djatout [5]

[1,2,3] Laboratory Of Semiconductor Devices Physic, University Of Tahri Mohamed, PB 417, Bechar (08000), Algeria
[1,2,3,4,5] Higher Normal School Of Bechar, Algeria

_____

Abstract: This work studies and simulates a thin film solar cell based on the InGaN material. The single-junction n/p $In_{0.622}Ga_{0.378}N$ (Eg = 1.39 eV) solar cell is the optimal structure found under normalized conditions (AM1.5G, 300K), we exhibit a comparison between three types of cells, with Lambertinne reflectors, textured reflectors, and flat reflectors to study optimum efficiency. The conversion efficiency increased from 16.46% with flat reflectors to18.67%. with textured reflectors, the solar cell exhibits a maximum efficiency of around 19.80 % with Lambertinne reflectors. The investigation results show that the $In_{0.622}Ga_{0.378}N$ with Lambertinne reflectors solar cell was inversely proportional to the temperature. The optimum concentration for doping for the donor is 5e17 cm^{-3} and for the acceptor is 5e17 cm^{-3}.
Keywords: Solar Cell, $In_{0.622}Ga_{0.378}N$, Simulation, Reflector, Temperature.

1. Introduction

The InGaN alloy is a promising candidate for photovoltaic applications because it exhibits attractive photovoltaic properties such as high tolerance to radiation, high mobility, and large absorption coefficient allowing thinner layers of material to absorb most of the solar spectrum[1]. This material has very good electronic properties the most important advantage of InGaN alloy might be the direct band gap energy which can be adjusted according to the indium composition. The energy band gap can be tuned from 0.7 eV to 3.42 eV, covering approximately the total solar spectrum. Our work aims to compare and improve solar cell performance using the simulation model in the Matlab simulation program to solve the Poisson equation; linking the load to the electrostatic potential, and the electrons continuity equations and holes. The basic solar cell performance parameters are the photocurrent density Jph, the open-circuit voltage Voc, the fill factor FF and the efficiency η. These parameters are briefly discussed.

2. Theoretical model

A compact summation method based on the simple case of a homo-junction with nonzero front and rear reflectivity to produce a full solution to the analytical model, examining both reflections. In principle, All the relationships used in this model are in references[2], [3]. Fig. 1 shows the layer structure for the cell. The thicknesses of the quasi-neutral region in the emitter and the base are denoted d_1 and d_2 respectively. The depletion thickness is **w**. The reflectivity of the front and rear surfaces of the solar cell are denoted R_1 [4]and R_2 respectively and the total thickness of the solar cell is the sum of the *n*-type QNR, the depletion region and the *p*-type QNR, $P = d_1 + w + d_2$.

Fig. 1 – Schematic diagram of the layer structure of the solar cell model
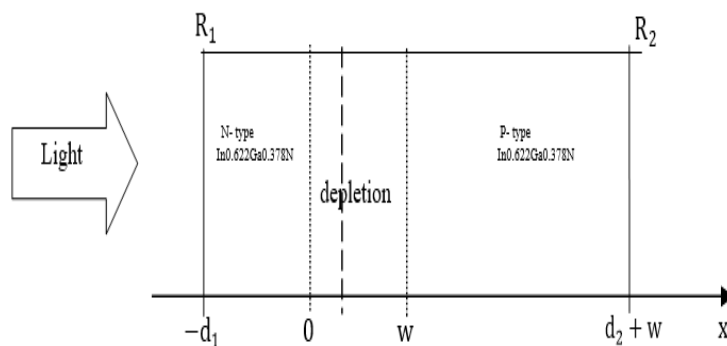
2.1 Photocurrent density

The density of the photocurrent is given by [5]:

$$J_{ph}(\lambda) = J_{p,ph}(d_1) + J_{n,ph}(d_2) + J_{dr,ph}(w) \qquad \text{------------ (1)}$$

$J_{p,ph}$ the hole current density, $J_{n,ph}$ the emitter current density, $J_{dr,ph}$ the depletion current density. In this simulation, The $In_{0.622}Ga_{0.378}N$ alloys absorption coefficient α is given by [6]:

$$\alpha(In_xGa_{1-x}N) = 10^5\sqrt{C(E_{ph} - E_g) + D(E_{ph} - E_g)^2} \qquad \text{---------------- (2)}$$

Where E_{ph} is the photon energy. C and D are coefficients, the equations of calculation coefficients are given in ref [7]. These parameters are dependent on the indium composition. The band gap energy $In_{0.622}Ga_{0.378}N$ alloy with a band gap energy of 1.39 eV, which is related to the indium composition fraction (x) at a temperature of 300 K by ref [8] [9]:

$$E_g(In_xGa_{1-x}N) = x.E_g^{InN} + (1-x).E_g^{GaN} - b.x.(1-x) \qquad \text{----------- (3)}$$

Where the band gap energy of InN E_g^{InN}, GaN E_g^{GaN} is 0.7 eV and 3.42 eV, respectively. x is the indium content, and b is the bowing parameter (b=1.43eV) [10], [11].

The dependence of the energy band gap on the temperature is as follows:

$$E_g(T) = E_g(0) - \frac{aT^2}{T+B} \qquad \text{---------------------- (4)}$$

$E_g(0)$ The energy gap of the material at 0K (eV), a an empirical constant (eV/K), B constant associated with the Debye temperature (K). All Varshni parameters and energy gaps at 0K and 300K , about the GaN and the InN are given in ref [12][8]. A detailed discussion of the specific assumptions used and a full derivation can be found in Fonash [2], and only the result is presented.

D_n and D_p are the electron and hole minority carrier diffusion coefficients, $L_n = (D_n\tau_n)^{0.5}$ and $L_p = (D_p\tau_p)^{0.5}$, τ_n and τ_p are the electron and hole minority carrier lifetime, S_n and S_p are the fronts and rear surfaces recombination velocities of the solar cell all these parameters are defined in ref [8], [13]. The other physical and optical parameters: N_A, N_D are acceptor and donor doping concentrations, n_i intrinsic carrier concentration in a semiconductor under thermodynamic equilibrium conditions, χ electron affinity, μ_n, μ_p The electron and hole mobility, all relationships depend on the temperature as given in the ref [10], [14], [15]. The refractive index model is given by the following equation [8], [14]:

$$n(E) = \sqrt{A * \left(\frac{E_{ph}}{E_g}\right)^{-2}\left\{2 - \sqrt{1 + \frac{E_{ph}}{E_g}} - \sqrt{1 - \frac{E_{ph}}{E_g}}\right\} + B} \qquad \text{--------------- (5)}$$

Where A and B depend on the indium composition. In the case of the $In_xGa_{1-x}N$ alloy, A and B are given by the following equation [1], [10][14]

$$A^{InGaN} = 13.55.x + 9.31(1-x) \qquad \text{--------------------- (6)}$$

$$B^{InGaN} = 2.05.x + 3.03(1-x) \qquad \text{------------------- (7)}$$

2.2 The dark current density

The dark current density is much detailed and given by:

$$J_d = J_s + J_{SRH} \qquad \text{--------------------- (8)}$$

$$J_s(\lambda) = J_{p,d}(d_1) + J_{n,d}(d_2) \qquad \text{---------------(9)}$$

$J_{p,d}$ the dark hole current density, $J_{n,d}$ the dark emitter current density, and J_{SRH} the dark current in the depletion region. The dark depletion current density was assumed to be dominated by Shockley–Read–Hall recombination [2], [5]. The overall minority carrier lifetime is then:

$$\frac{1}{\tau} = \frac{1}{\tau_r} + \frac{1}{\tau_{SRH}} \qquad \text{--------------------- (10)}$$

With τ_r is the radiative lifetime of minority carriers and τ_{SRH} is the overall minority carrier Shockley-Read-Hall lifetime [16], [17]

2.3 Open circuit voltage

The separation of charges sets up a forward potential difference between the two contacts of the solar cell, which under open-circuit conditions $(J = 0)$ is known as the open-circuit voltage Voc [2], [4].

2.4 Fill factor and conversion efficiency

The output power of P of solar cell is:

$$P = JV = (J_{ph} - J_d)V \qquad \text{-------------- (11)}$$

The maximum output power P_m can be derived using $\frac{dP}{dV} = 0$.

$$P = J_mV_m = J_{ph}\left[V_m - V_T\left(1 + \ln\left(1 + \frac{V_m}{V_T}\right)\right)\right] \qquad \text{--------------- (12)}$$

Where J_m and V_m is the maximum current density and maximum voltage, and V_m can be calculated numerically from the following equation:

$$V_m \approx V_{oc} - V_T\left(1 + \ln\left(1 + \frac{V_m}{V_T}\right)\right) \qquad \text{--------------- (13)}$$

The fill factor FF and the conversion efficiency η of the cell is defined as:

$$FF = \frac{J_m V_m}{J_{ph}.V_{oc}} \qquad \text{----------------- (14)}$$

$$\eta = \frac{J_{ph}.V_{oc}.FF}{P_{in}} \qquad \text{---------------- (15)}$$

Where P_{in} is the incident power of the solar spectrum $P_{in} = 1353 w/m^2$.

3 Result and discussion

3.1 Solar cell structure details

Our reference structure is a single-junction solar cell based on $In_{0.622}Ga_{0.378}N$, The published InGaN solar cell design is found in[18], [19]. Fig. 2 shows the structure of the cell used in the simulation. The simulation was carried out under the illumination of global AM1.5. The InGaN material used in our work is defined from its parameters taken from the reference[10], [19], their initial physical and geometrical parameter values used are collected in table 1.

Fig. 2 – shows the structure of the cell used in the simulation
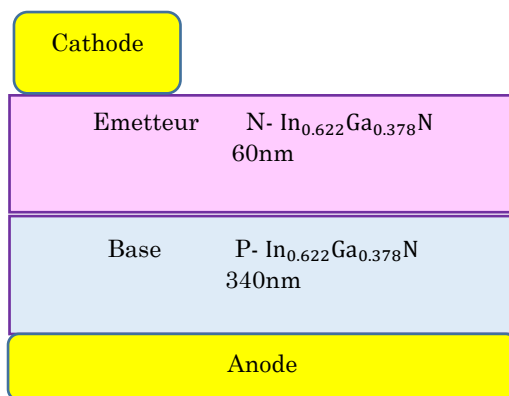
Table 1- Parameters used to simulate of $In_{0.622}Ga_{0.378}N$ solar cell under T=300k [10], [19]

Parameters	$In_{0.622}Ga_{0.378}N$
The thickness of the emitter (nm)	60
The Thickness of the base (nm)	340
Band gap E_g (ev)	1.39
Donor concentration (cm^{-3})	5e17
Acceptor concentration (cm^{-3})	5e17
S_n and S_p the fronts and rear surfaces recombination velocities (cm/s)	1e3

3.2 Comparison between three cases and Optimal Performance of $In_{0.622}Ga_{0.378}N$

We study three cases of the cell $In_{0.622}Ga_{0.378}N$ based, each of these cells had a reflector to assure light trapping, this reflector increases the trajectory length of the luminous to the extinction. The first cell has Lambertinne reflectors, the second with textured reflectors, and the third flat reflectors. The calculated electrical parameters:J_{ph}, V_{oc}, η, FF, P_{max}, and the J(V) curve of three cases, were presented, respectively, in fig 3 and table 2 .

The results he obtained are the best, the cell with Lambertinne reflection produces improvements on the device and produces more photocurrent compared to the cells with textured and flat reflectors, this increase is logical because the reflector increases the light path and makes it longer in the cell.

Fig. 3 –shows curves solar cells' characteristic of J = f (V).
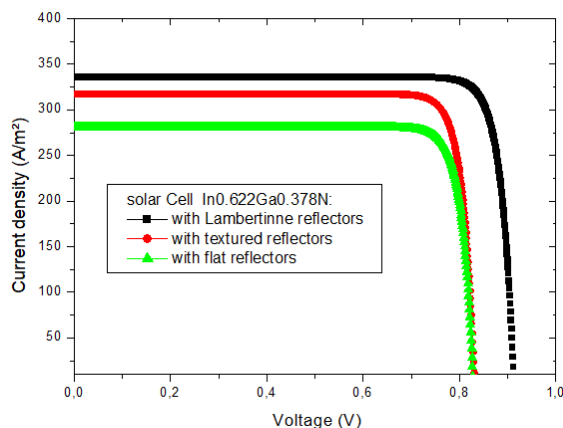
Table 2 – The calculated electrical parameters of solar cells in different cases.

PV parameters	η %	$J_{ph}(A/m^2)$	FF	V_{oc}	$P(W/m^2)$
Reflectors Lambertinne	19.80	335.75	0.8751	0.9119	267.94
Reflector textured	18.67	317.10	0.8750	0.9104	252.60
Reflector flat	16.46	280.70	0.8015	0.9073	222.75

The curves spectral response for three cases of solar cells are presented in fig 4.

Fig. 4- show the curves spectral response of solar cells.
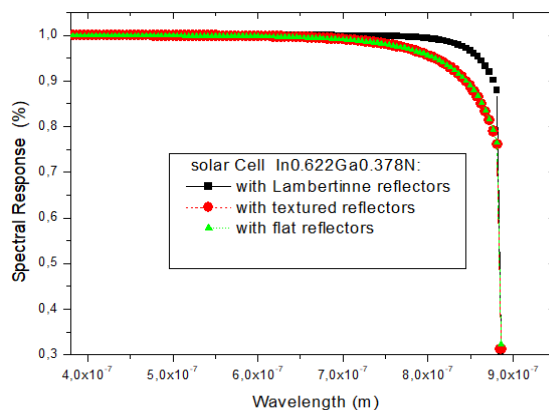
Improving the wavelength to spectral response is visible, with pronounced fringes in the solar cell with a lambertinne reflectors due to the interference of forward and reverse propagation in the structure.

3.3 The effect of the temperature on the optimal solar cell

To study the optimum performance, we simulated the solar cell with a reflector lambertinne inverter at 280, 300, 320, 340 and 400 K. As the results of these simulations are shown in Table 3.

Table 3 – parameters of the different values

PV parameter	280	300	320	340	400
η %	20,85	19,80	18,76	17,71	13,35
$P(W/m^2)$	282,08	267,94	253,80	239,58	180,63
$J_{ph}(A/m^2)$	340,75	335,75	330,75	299,75	295,75
V_{oc}	1,02	0,91	0,82	0,74	0,54
FF	0,83	0,87	0,82	0,76	0, 75

calculated electrical solar cell at temperatures.

The curves for the efficiency, maximum power, photo-current, open circuit tension, and fill factor, all dependent on the temperature are shown in fig 5, fig 6, fig 7, fig 8, and fig 9 respectively.

Efficiency decreases by approximately 1% for every 20 k increase in temperature. The efficiency versus temperature plot in Figure 5 is a visual illustration of this.

Fig. 5- show the curve of the efficiency versus temperature of a solar cell.
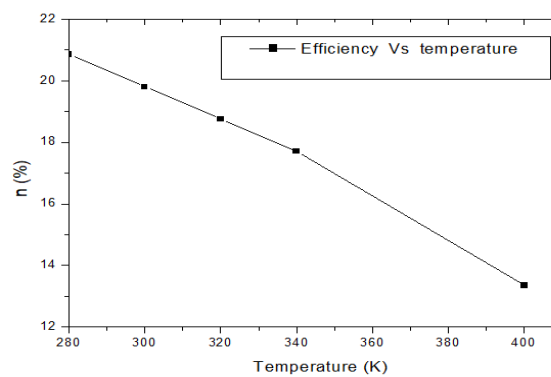
The decrease in solar cell efficiency and maximum power is mainly due to voltage drop.

Fig. 6- show the curve of the maximum power versus temperature of a solar cell.
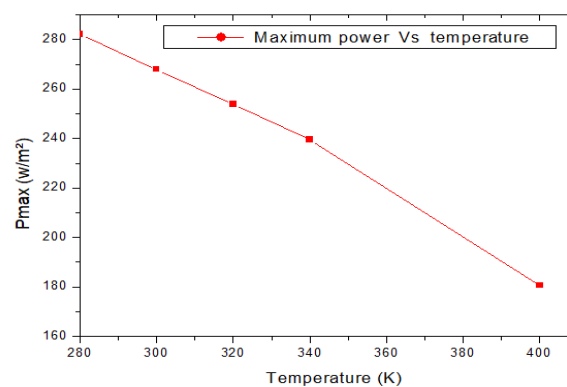
This decrease in voltage is not surprising, as it is expected to be about 0.9 v/k for the model performance of the solar cell, which is less than 0.1 volts per increase of 20 km in temperature.

Fig.7- show the curve of open circuit voltage versus the temperature of a solar cell.
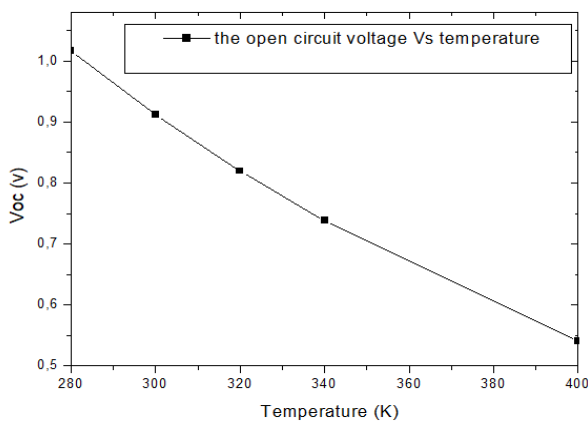
The short circuit current remains decreases, as expected, and is illustrated in the plot of this parameter in Figure 8.

Fig.8- show the curve of the photo-current versus temperature of a solar cell.
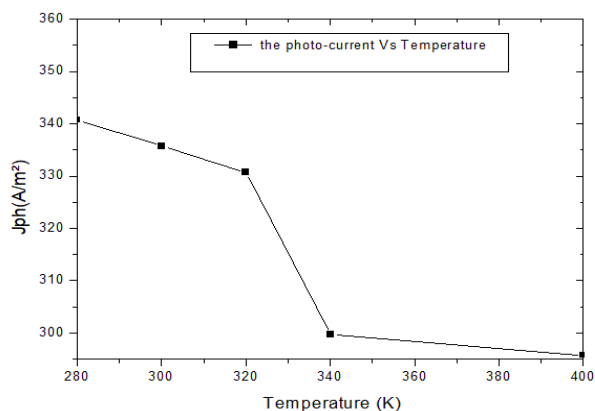
The FF increases an average by 0.04 for every 20 K increase in the temperature. A plot of the FF versus temperature is presented in Figure 9.

Fig.9- show the curve of the fill factor versus temperature of a solar cell.
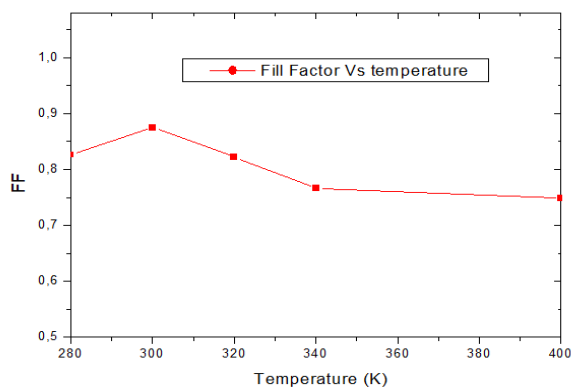
The results of the temperature simulator are important because the solar cells are required to work at high temperatures and not near room temperature, or 300 k°.

3.4 Effect of doping concentrations on the performance of the solar cell

We study the effect of Nd and Na concentration, changing the doping concentration of the emitter and the base at $1e^{16}cm^{-3}$, $1e^{17}cm^{-3}$, $1e^{18}cm^{-3}$, and $1e^{19}cm^{-3}$. we obtain the results in fig 10, fig 11, fig 12, and fig 13 respectively.

Fig. 10- show the curve of efficiency versus the doping concentrations of a solar cell.
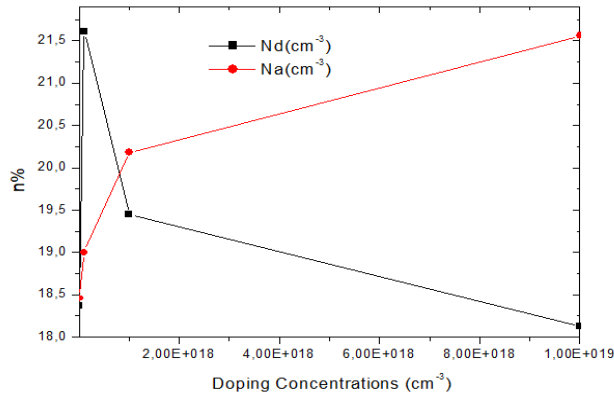
Fig. 11- show the curve of open circuit voltage versus the doping concentrations of a solar cell.
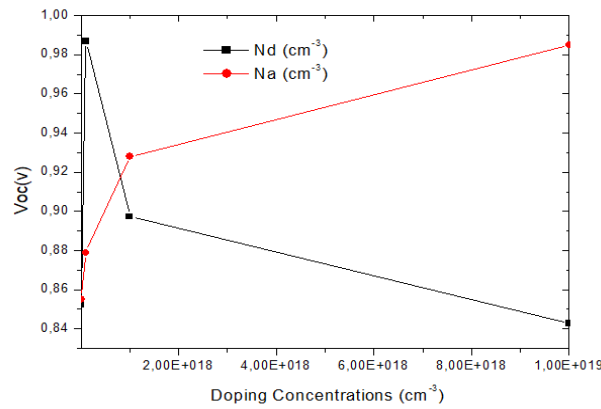
Fig. 12- show the curve of fill factor versus the doping concentrations of a solar cell.
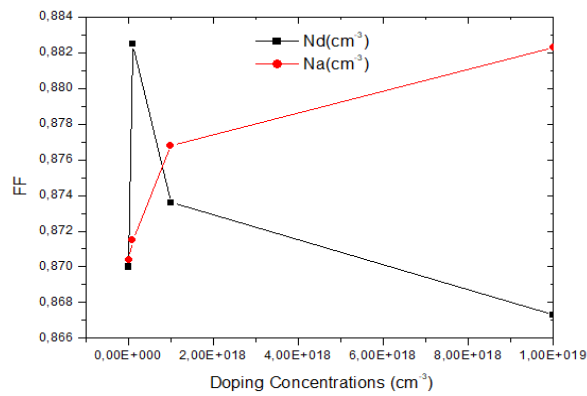
Fig. 13- show the curve of photo-current versus the doping concentrations of a solar cell.
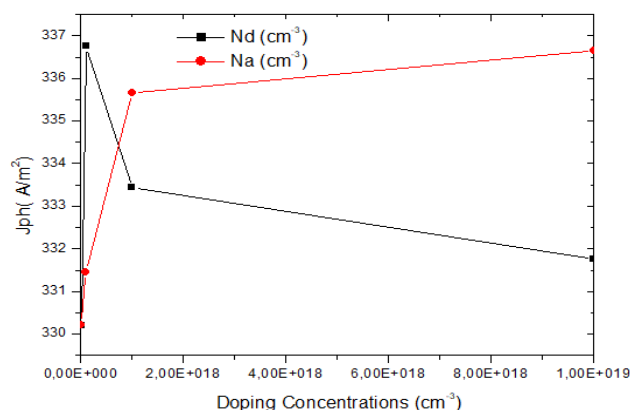
With increasing concentration doping Nd all parameters first increase and then decrease. but with the increase of the doping concentration Na all characteristics increase. The optimum doping of solar cell is reached when the acceptor doping concentration is 5e17 cm^{-3} and the donner doping concentration is 5e17 cm^{-3}.

4. CONCLUSION

This article analyzes the effect of different techniques the light trapping on the performance of n/p solar cells. An $In_{0.622}Ga_{0.378}N$ junction cell serves as the model of this analysis. we use MATLAB to model this cell and simulate its behavior. The cell's performance under the effect of temperature was evaluated at 275, 300, 325, 350, 375, and 400 K. And doping concentrations at: 1e^{16}cm^{-3}, 1e^{17}cm^{-3}, 1e^{18}cm^{-3}, and 1e^{19}cm^{-3}. The simulations provide the results necessary to make observations about cell design and the effect of operating temperature. First, to improve in efficiency, we placed the Lambertinne reflector in the cell this is a technique of gard light trapping in the cell that makes the best optimum performance. Second, the obvious conclusion of these simulations is that as temperature increases, performance decreases. and thirdly, performance increases with increasing doping acceptor concentration. This is why it is important to have the expected design and temperature of a solar cell to guide the design process.

References

[1]   H. Movla, D. Salami, and S. V. Sadreddini, "Simulation analysis of the effects of defect density on the performance of p-i-n InGaN solar cell," *Appl. Phys. A Mater. Sci. Process.*, vol. 109, no. 2, pp. 497–502, 2012, doi: 10.1007/s00339-012-7062-8.

[2]   "Physics of semiconductor devices," *Choice Reviews Online*, vol. 27, no. 11. pp. 27-6393-27–6393, 1990, doi: 10.5860/choice.27-6393.

[3]   X. Chen, K. D. Matthews, D. Hao, W. J. Schaff, and L. F. Eastman, "solidi," vol. 1105, no. 5, pp. 1103–1105, 2008, doi: 10.1002/pssa.200778695.

[4]   R. M. Pujahari, *Crystalline silicon solar cells*. 2021.

[5]   M. P. Lumb *et al.*, "Extending the 1-d hovel model for coherent and incoherent back reflections in homojunction solar cells," *IEEE J. Quantum Electron.*, vol. 49, no. 5, pp. 462–470, 2013, doi: 10.1109/JQE.2013.2252148.

[6]   L. J.-H. Lin and Y.-P. Chiou, "Optical design of GaN/In_xGa_1-xN/cSi tandem solar cells with triangular diffraction grating," *Opt. Express*, vol. 23, no. 11, p. A614, 2015, doi: 10.1364/oe.23.00a614.

[7]   G. F. Brown, J. W. A. Iii, W. Walukiewicz, and J. Wu, "Solar Energy Materials & Solar Cells Finite element simulations of compositionally graded InGaN solar cells," *Sol. Energy Mater. Sol. Cells*, vol. 94, no. 3, pp. 478–483, 2010, doi: 10.1016/j.solmat.2009.11.010.

[8]   A. Abdoulwahab, S. Ould, S. Hamady, and N. Fressengeas, "Multivariate numerical optimization of an InGaN-based hetero junction solar cell," 2017.

[9]   J. O. F. Hit and S. S. Edition, "陈家喜1，2（1. ，" pp. 4–9, 2012.

[10]   A. Adaine, "Optimisation numérique de cellules solaires à très haut rendement à base d'InGaN Abdoulwahab Adaine To cite this version : HAL Id : tel-01870260 soutenance et mis à disposition de l'ensemble de la Contact : ddoc-theses-contact@univ-lorraine.fr," 2018.

[11]   M. Sarollahi, M. A. Aldawsari, R. Allaparthi, and M. A. Refaei, "Study of simulations of double graded InGaN solar cell structures," pp. 1–14.

[12]   M. B. Bouyeddou, M. A. Bensaad, M. A. Garadi, and M. A. Bouarfa, "Etude des performances d'une cellule photovoltaïques à base d'InGaN," 2018.

[13]   H. Vilchis, M. A. Vidal, and A. G. Rodríguez, "Complex refractive index of InXGa1-XN thin films grown on cubic (100) GaN/MgO," *Thin Solid Films*, vol. 626, no. 100, pp. 55–59, 2017, doi: 10.1016/j.tsf.2017.02.016.

[14]   L. A. Vilbois, A. Cheknane, A. Bensaoula, C. Boney, and T. Benouaz, "Simulation of a solar cell based on InGaN," *Energy Procedia*, vol. 18, pp. 795–806, Jan. 2012, doi: 10.1016/j.egypro.2012.05.095.

[15]   M. Farahmand *et al.*, "Monte Carlo simulation of electron transport in the III-nitride Wurtzite phase materials system: Binaries and ternaries," *IEEE Trans. Electron Devices*, vol. 48, no. 3, pp. 535–542, 2001, doi: 10.1109/16.906448.

[16]   G. F. Brown, J. W. Ager, W. Walukiewicz, and J. Wu, "Finite element simulations of compositionally graded InGaN solar cells," *Sol. Energy Mater. Sol. Cells*, vol. 94, no. 3, pp. 478–483, Mar. 2010, doi: 10.1016/J.SOLMAT.2009.11.010.

[17]   S. Feng, C. Lai, C. Tsai, Y. Su, and L. Tu, "Modeling of InGaN p-n junction solar cells," vol. 3, no. 10, pp. 1777–1788, 2013, doi: 10.1364/OME.3.001777.

[18]   A. Mesrane, F. Rahmoune, A. Mahrane, and A. Oulebsir, "Design and Simulation of InGaN ? - ? Junction Solar Cell," vol. 2015, 2015.

[19]   O. Signaux, "Magister en Electronique Modélisation des cellules solaires en InGaN en utilisant Atlas Silvaco . Yacine MAROUF Devant le jury composé de :"